

TEST-TIME ITERATIVE ERROR CORRECTION FOR EFFICIENT DIFFUSION MODELS

Yunshan Zhong¹, Weiqi Yan², Yuxin Zhang²

¹School of Computer Science and Technology, Hainan University

²MAC Lab, Department of Artificial Intelligence, School of Informatics, Xiamen University

yszhong01@gmail.com, weiqi-yan@outlook.com, yuxinzhang@stu.xmu.edu.cn

ABSTRACT

With the growing demand for high-quality image generation on resource-constrained devices, efficient diffusion models have received increasing attention. However, such models suffer from approximation errors introduced by efficiency techniques, which significantly degrade generation quality. Once deployed, these errors are difficult to correct, as modifying the model is typically infeasible in deployment environments. Through an analysis of error propagation across diffusion timesteps, we reveal that these approximation errors can accumulate exponentially, severely impairing output quality. Motivated by this insight, we propose Iterative Error Correction (IEC), a novel test-time method that mitigates inference-time errors by iteratively refining the model’s output. IEC is theoretically proven to reduce error propagation from exponential to linear growth, without requiring any retraining or architectural changes. IEC can seamlessly integrate into the inference process of existing diffusion models, enabling a flexible trade-off between performance and efficiency. Extensive experiments show that IEC consistently improves generation quality across various datasets, efficiency techniques, and model architectures, establishing it as a practical and generalizable solution for test-time enhancement of efficient diffusion models.

1 INTRODUCTION

Diffusion models Ho et al. (2020); Rombach et al. (2022); Nichol & Dhariwal (2021) have achieved state-of-the-art generative performance across a wide range of tasks, including image synthesis Song et al. (2020b); Choi et al. (2021); Saharia et al. (2022a); Tumanyan et al. (2023); Li et al. (2022); Saharia et al. (2022c); Gao et al. (2023); Avrahami et al. (2022); Kawar et al. (2023); Meng et al. (2021), text-to-image generation Nichol et al. (2021); Ramesh et al. (2022); Saharia et al. (2022b); Zhang et al. (2023b), text-to-3D generation Lin et al. (2023); Luo & Hu (2021); Poole et al. (2022), video generation Mei & Patel (2023), and audio generation Huang et al. (2022); Zhang et al. (2023a). However, diffusion models typically require hundreds of iterative denoising steps and contain billions of parameters, resulting in high computational costs that hinder deployment in resource-constrained environments. To address this limitation, extensive efficiency techniques have been devoted to developing efficient model techniques for diffusion models Song et al. (2020a); Zhang et al. (2022); Zheng et al. (2023); Liu et al. (2025b); Shang et al. (2023); Li et al. (2023; 2024c).

Among these techniques, network quantization Shang et al. (2023); Li et al. (2023; 2024c); Zheng et al. (2024) and feature caching Chen et al. (2024b); Zou et al. (2024); Ma et al. (2024b) have emerged as two promising approaches. The former reduces data precision to low-bit representations to simultaneously shrink model size and accelerate inference, while the latter caches intermediate features to eliminate redundant computations across diffusion timesteps. Although these methods effectively reduce overhead, they inevitably suffer from approximation errors between the efficient model and the original counterpart, which degrade the generation quality of the model. Prior studies have attempted to mitigate such errors through specialized mechanisms. For example, timestep-wise quantization parameters Wang et al. (2023); Liu et al. (2024b) have been introduced to capture the dynamics of time-varying activations, while non-uniform caching strategies Ma et al. (2024b) exploit similarity patterns between adjacent timesteps to improve performance. Despite their effectiveness,

these methods remain pre-deployment solutions that require the ability to re-execute the model-efficiency pipeline and the original model.

In practice, such requirements often do not hold once a model has been deployed in edge or production environments. On the one hand, reapplying the model-efficiency pipeline and redeploying the model incurs significant engineering overhead, making it impractical in many cases. Also, deployed models are typically immutable due to storage limitations, deployment policies, or system design constraints. On the other hand, after being deployed, the original model is often irretrievable, making re-executing the model-efficiency pipeline unfeasible. For instance, a quantized model may no longer retain its original high-precision weights, making re-quantization infeasible. Inspired by recent advances in test-time scaling Snell et al. (2024); Lightman et al. (2023); Muennighoff et al. (2025); Ma et al. (2025); Singhal et al. (2025); Prabhudesai et al. (2023); Xiao & Snoek (2024), where model behavior is adjusted at inference time without retraining, we ask: *Is it possible to improve the performance of an already deployed diffusion model without repeating the model-efficiency pipeline?*

To answer this question, we begin by analyzing how errors propagate through diffusion timesteps and reveal that they accumulate exponentially, which significantly degrades the final generation quality. Motivated by this finding, we propose Iterative Error Correction (IEC), a novel test-time method that mitigates these errors by iteratively refining the model’s output. Theoretically, we show that IEC reduces error accumulation from exponential to linear growth. IEC is a plug-and-play method that operates entirely at test-time. It requires no re-running the model-efficiency pipeline, no fine-tuning weights, and no changes in model architecture, making it compatible with deployed diffusion models. While IEC introduces additional computational overhead, it is highly flexible and can be selectively applied to a subset of all diffusion timesteps. Applying IEC to more timesteps yields greater quality improvements, while using fewer timesteps reduces computational overhead. Skipping IEC entirely preserves the model’s original performance. This flexibility provides users with fine-grained control over the trade-off between efficiency and generation quality, depending on resource constraints and application needs. By enhancing the performance of efficient diffusion models in deployment, IEC preserves the compatibility and reusability of these models, making it a practical and generalizable solution for real-world applications.

2 RELATED WORK

2.1 DIFFUSION MODEL

Diffusion models Ho et al. (2020); Rombach et al. (2022) consist of *forward process* and *reverse process*. In the *forward process*, given input data distribution $x_0 \sim q(x)$, diffusion models add a series of Gaussian noise to x_0 to resulting in a sequence of noisy samples $x_t, 0 \leq t \leq T$:

$$q(x_{1:T}|x_0) = \prod_{t=1}^T q(x_t|x_{t-1}), \quad (1)$$

$$q(x_t|x_{t-1}) = \mathcal{N}(x_t; \sqrt{\alpha_t}x_{t-1}, \beta_t \mathbf{I}),$$

where $\alpha_t = 1 - \beta_t$, β_t is t -based parameters. In the *reverse process*, given randomly sampled Gaussian noise $x_T \sim \mathcal{N}(\mathbf{0}, \mathbf{I})$, diffusion models progressively generate images by:

$$p_\theta(x_{t-1}|x_t) = \mathcal{N}(x_{t-1}; \hat{\mu}_{\theta,t}(x_t), \hat{\beta}_t \mathbf{I}). \quad (2)$$

For DDIM Song et al. (2020a), the $\hat{\beta}_t = 0$ and $\hat{\mu}_{\theta,t}$ is defined by:

$$x_{t-1} = \sqrt{\alpha_{t-1}} \frac{x_t - \sqrt{1 - \alpha_t} \epsilon_\theta(x_t, t)}{\sqrt{\alpha_t}} + \sqrt{1 - \alpha_{t-1}} \epsilon_\theta(x_t, t). \quad (3)$$

2.2 EFFICIENT DIFFUSION

Significant efforts have been devoted to developing efficient diffusion models, which can be broadly categorized into two types: temporal efficiency and structural efficiency Liu et al. (2025b). Temporal efficiency methods focus on reducing the number of sampling timesteps. For instance, methods such as DDIM Song et al. (2020a) and GDDIM Zhang et al. (2022) modify the denoising equations

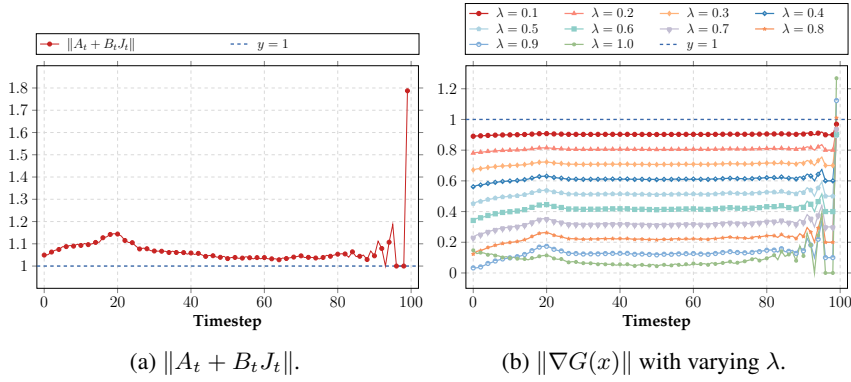


Figure 1: Empirical results of (a) $\|A_t + B_t J_t\|$; (b) $\|\nabla G(x)\|$ under varying λ . Reported values are averaged over 100 sample generations using a DDIM pretrained on CIFAR-10.

to enable fewer sampling steps, while others Zheng et al. (2023); Shih et al. (2023) accelerate inference by performing multiple denoising timesteps in parallel. DistriFusion Li et al. (2024a) further improves efficiency by dividing input patches across multiple GPUs. Additionally, fast solvers for diffusion Liu et al. (2022); Dockhorn et al. (2022); Yin et al. (2024b;a); Lu et al. (2022a;b) have been proposed to reduce the computational overhead associated with sampling. Structural efficiency methods, on the other hand, aim to reduce model complexity and are complementary to temporal efficiency techniques, making them increasingly popular. For example, network quantization has emerged as a key approach for efficient diffusion model Li et al. (2024c); Zheng et al. (2024); Yang et al. (2024); Deng et al. (2025); Zhao et al. (2024); Huang et al. (2024a); Chen et al. (2024a); Dong & Zhang (2025). Quantization-aware training (QAT) Li et al. (2024c); Zheng et al. (2024) restores model performance at low bit-widths but incurs significant training overhead. In contrast, post-training quantization (PTQ) Shang et al. (2023); Li et al. (2023); Wu et al. (2024a) requires minimal computational resources and small calibration datasets, making it more suitable for scenarios with limited resources. PTQ4DM Shang et al. (2023) and Q-Diffusion Li et al. (2023) introduced time-aware calibration to realize quantized diffusion models. Subsequent works have refined these methods by addressing quantization error, feature re-balancing, calibration data collection, model reconstruction, mixed-precision strategies, and so on He et al. (2024); Huang et al. (2024b); Wang et al. (2024a;b); Feng et al. (2025); Liu et al. (2024c); Sun et al. (2024); Wu et al. (2024b). Moreover, techniques such as LoRA-based optimization Hu et al. (2021) have been applied to further enhance quantized diffusion models Li et al. (2024b); He et al. (2023). In addition to quantization, feature caching has also gained attention Chen et al. (2024b); Zou et al. (2024); Ma et al. (2024b); Wimbauer et al. (2024); Liu et al. (2025a; 2024a); Ma et al. (2024a). These methods aim to reduce inference time by reusing pre-computed features across diffusion steps. Recent studies, such as CacheQuant Liu et al. (2025b), combine caching with quantization to achieve even greater efficiency. Other structural efficiency techniques include token pruning Fang et al. (2024) and sparsity Fan et al. (2025). In this work, we focus on mitigating the errors introduced by structural efficiency methods.

3 METHOD

3.1 ANALYSIS OF ERROR ACCUMULATION IN EFFICIENT DIFFUSION MODELS

In this subsection, we present a theoretical analysis of error propagation and accumulation across diffusion timesteps, using the deterministic DDIM sampling procedure as an example.

Preliminaries. We consider the deterministic DDIM sampling process defined as:

$$x_{t-1} = \sqrt{\alpha_{t-1}} \frac{x_t - \sqrt{1 - \alpha_t} \epsilon_\theta(x_t, t)}{\sqrt{\alpha_t}} + \sqrt{1 - \alpha_{t-1}} \epsilon_\theta(x_t, t). \quad (4)$$

For brevity of notation, we define the following coefficients:

$$A_t = \frac{\sqrt{\alpha_{t-1}}}{\sqrt{\alpha_t}}, \quad B_t = \sqrt{1 - \alpha_{t-1}} - \sqrt{\alpha_{t-1}} \frac{\sqrt{1 - \alpha_t}}{\sqrt{\alpha_t}}, \quad (5)$$

thereby simplifying the rule to:

$$x_{t-1} = A_t x_t + B_t \epsilon_\theta(x_t, t). \quad (6)$$

Modeling Error. In efficient diffusion model methods, such as quantized or cached models, two primary types of errors are introduced at each timestep. First, due to error propagation from the previous timestep, there exists a discrepancy δ_t between the perturbed input \tilde{x}_t and the ideal input x_t , defined as $\tilde{x}_t = x_t + \delta_t$. Second, perturbations from network quantization or feature caching introduce an error ϵ_θ^δ in the model's prediction. Specifically, the perturbed prediction $\tilde{\epsilon}_\theta(x_t, t)$ differs from the ideal case $\epsilon_\theta(x_t, t)$ is defined as $\tilde{\epsilon}_\theta(x_t, t) = \epsilon_\theta(x_t, t) + \epsilon_\theta^\delta$.

Incorporating these errors, the perturbed update rule at timestep t becomes:

$$\begin{aligned} \tilde{x}_{t-1} &= A_t \tilde{x}_t + B_t \tilde{\epsilon}_\theta(\tilde{x}_t, t) \\ &= A_t(x_t + \delta_t) + B_t \tilde{\epsilon}_\theta(x_t + \delta_t, t) \\ &\approx A_t(x_t + \delta_t) + B_t(\tilde{\epsilon}_\theta(x_t, t) + J_t \delta_t) \\ &= A_t(x_t + \delta_t) + B_t(\epsilon_\theta(x_t, t) + \epsilon_\theta^\delta + J_t \delta_t), \end{aligned} \quad (7)$$

where the approximation uses the first-order Taylor expansion, and $J_t = \frac{\partial \tilde{\epsilon}_\theta(x, t)}{\partial x} \big|_{x=x_t}$ represents the Jacobian of the model output with respect to its input.

Error Propagation. By subtracting the ideal update in Eq. 6 from the perturbed update in Eq. 7, we derive the recursive relation for error propagation:

$$\begin{aligned} \delta_{t-1} &= \tilde{x}_{t-1} - x_{t-1} \\ &\approx A_t \delta_t + B_t(\epsilon_\theta^\delta + J_t \delta_t) \\ &= (A_t + B_t J_t) \delta_t + B_t \epsilon_\theta^\delta. \end{aligned} \quad (8)$$

Recursively expanding Eq. 8 from timestep T to 0, and assuming the initial error $\delta_T = 0$ (since x_T is drawn from an ideal Gaussian prior), the accumulated error at $t = 0$ is given by:

$$\delta_0 = \sum_{i=1}^T \left(\prod_{j=i+1}^T (A_j + B_j J_j) \right) (B_i \epsilon_\theta^\delta). \quad (9)$$

Eq. 9 reveals that the final error δ_0 is a weighted sum of per-timestep prediction errors, where each contribution is scaled by the product of the matrices $(A_j + B_j J_j)$ from timestep $i + 1$ to T .

Analysis of Error Growth. To understand whether the propagated error amplifies or decays over time, we analyze the spectral norm $\|A_t + B_t J_t\|$, which quantifies the maximum amplification of the linear transformation at each timestep. Specifically, if $\|A_t + B_t J_t\| > 1$, the corresponding error component is amplified, and the error can grow exponentially if such amplification persists, leading to instability. In contrast, if $\|A_t + B_t J_t\| < 1$ for all t , the propagated error decays over time, indicating a relatively stable and robust sampling process. Empirical observations, as shown in Fig. 1a, demonstrate that $\|A_t + B_t J_t\|$ consistently exceeds 1 across timesteps, suggesting that the errors introduced by efficient diffusion methods tend to accumulate exponentially, posing a challenge in stability.

As shown in Eq. 9, the key to reducing error lies in breaking the exponential growth trend during the accumulation process. In the following subsection, we propose a novel and effective method that transforms the error growth from exponential to linear.

3.2 ITERATIVE ERROR CORRECTION

To mitigate error accumulation, we introduce Iterative Error Correction (IEC), a theoretically motivated, plug-and-play method designed to reduce error accumulation from exponential to linear growth at test-time. The core idea of IEC is to introduce correction steps within diffusion timesteps. Specifically, at a timestep $t - 1$, an initial estimate $x_{t-1}^{(0)}$ is computed using the standard DDIM update defined in Eq. 6: $x_{t-1}^{(0)} = A_t x_t + B_t \epsilon_\theta(x_t, t)$. We then iteratively refine this estimate by repeatedly applying the following update rule:

$$x_{t-1}^{(k+1)} = x_{t-1}^{(k)} + \lambda \left(A_t x_t + B_t \epsilon_\theta(x_{t-1}^{(k)}, t) - x_{t-1}^{(k)} \right), \quad k = 0, 1, 2, \dots, \quad (10)$$

where λ is a tunable hyperparameter. The iteration proceeds until the difference $\|x_{t-1}^{(k+1)} - x_{t-1}^{(k)}\|$ falls below a predefined threshold or the maximum number of iterations is reached, yielding the final estimate x_{t-1}^* .

Convergence Analysis. We provide a mathematical justification for the convergence of IEC using fixed-point theory. Eq. 10 can be reformulated as:

$$x_{t-1}^{(k+1)} = (1 - \lambda)x_{t-1}^{(k)} + \lambda \left(A_t x_t + B_t \epsilon_\theta(x_{t-1}^{(k)}, t) \right). \quad (11)$$

This allows us to define the mapping $G(x)$ as:

$$G(x) = (1 - \lambda)x + \lambda \left(A_t x_t + B_t \epsilon_\theta(x, t) \right). \quad (12)$$

The iterative procedure in Eq. 10 is thus equivalent to applying fixed-point iteration to solve:

$$x_{t-1}^* = G(x_{t-1}^*). \quad (13)$$

According to Banach's fixed-point theorem Banach (1922), the iterative procedure converges to a unique fixed point x_{t-1}^* if the mapping $G(x)$ is a contraction mapping, *i.e.*, there exists a Lipschitz constant $0 < L < 1$ such that:

$$\|G(x) - G(y)\| \leq L\|x - y\|, \forall x, y. \quad (14)$$

To estimate the Lipschitz constant L , we compute the Jacobian of $G(x)$:

$$\nabla G(x) = (1 - \lambda)I + \lambda B_t J_t, \quad (15)$$

where J_t is the Jacobian matrix. Then, the Lipschitz constant L is given by:

$$L = \|\nabla G(x)\| = \|(1 - \lambda)I + \lambda B_t J_t\|. \quad (16)$$

To guarantee convergence, it is necessary to satisfy $0 < L < 1$. Since $B_t < 0$, an appropriately chosen positive λ reduces the Lipschitz constant L via the term $\lambda B_t J_t$, ensuring $L < 1$. Empirically, as shown in Fig. 1b, we observe that setting λ within the range $[0.1, 0.7]$ consistently ensures that $\|\nabla G(x)\| < 1$ across all timesteps. In this paper, we set λ to 0.5 as a practical choice based on these observations. Moreover, since $G(x)$ is continuously differentiable, Eq. 14 holds by the Mean Value Inequality for vector-valued functions Munkres (2018), confirming that G is a contraction mapping and IEC can converge to the fixed-point solution.

Error Accumulation in IEC. The proposed IEC effectively suppresses error accumulation. To demonstrate this, we define the error at iteration $k + 1$ of IEC as:

$$\begin{aligned} \delta_{t-1}^{(k+1)} &= x_{t-1}^{(k+1)} - x_{t-1} = G(x_{t-1}^{(k)}) - x_{t-1} \\ &= \underbrace{G(x_{t-1} + \delta_{t-1}^{(k)}) - G(x_{t-1})}_{\text{first term}} + \underbrace{G(x_{t-1}) - x_{t-1}}_{\text{second term}}, \end{aligned} \quad (17)$$

where $\delta_{t-1}^{(k)} = x_{t-1}^{(k)} - x_{t-1}$ is the accumulated error at iteration k . The first term of Eq. 17 can be approximated by $G(x_{t-1} + \delta_{t-1}^{(k)}) - G(x_{t-1}) \approx \nabla G \cdot \delta_{t-1}^{(k)}$.

By considering the noisy input and noisy model prediction, the mapping $G(x)$ is defined as:

$$G(x) = (1 - \lambda)x + \lambda(A_t \tilde{x}_t + B_t \tilde{\epsilon}_\theta(x, t)), \quad (18)$$

where $\tilde{x}_t = x_t + \delta_t$ and $\tilde{\epsilon}_\theta(x, t) = \epsilon_\theta(x, t) + \epsilon_\theta^\delta$ represent the noisy input and noisy model prediction, respectively. Consequently, the second term in Eq. 17 can be approximated by:

$$\begin{aligned} G(x_{t-1}) - x_{t-1} &= \\ (1 - \lambda)x_{t-1} + \lambda(A_t(x_t + \delta_t) + B_t(\epsilon_\theta(x_{t-1}, t) + \epsilon_\theta^\delta)) - x_{t-1} &= \\ = \lambda(A_t x_t + B_t \epsilon_\theta(x_{t-1}, t) - x_{t-1}) + \lambda(A_t \delta_t + B_t \epsilon_\theta^\delta) &= \\ = \lambda B_t(\epsilon_\theta(x_{t-1}, t) - \epsilon_\theta(x_t, t)) + \lambda(A_t \delta_t + B_t \epsilon_\theta^\delta), \end{aligned}$$

where the last equality uses the relationship $x_{t-1} = A_t x_t + B_t \epsilon_\theta(x_t, t)$. Taking the norm of $\delta_{t-1}^{(k+1)}$ and applying the triangle inequality, we obtain:

$$\begin{aligned} \|\delta_{t-1}^{(k+1)}\| &\leq \|\nabla G(x_{t-1}) \cdot \delta_{t-1}^{(k)}\| + \\ \lambda(\|B_t(\epsilon_\theta(x_{t-1}, t) - \epsilon_\theta(x_t, t))\| + \|A_t \delta_t + B_t \epsilon_\theta^\delta\|) &\leq L \|\delta_{t-1}^{(k)}\| + C, \end{aligned}$$

where $L = \|\nabla G(x_{t-1})\|$ is the Lipschitz constant, and $C = \lambda(\|B_t(\epsilon_\theta(x_{t-1}, t) - \epsilon_\theta(x_t, t))\| + \|A_t \delta_t + B_t \epsilon_\theta^\delta\|)$ is a bounded constant independent of $\delta_{t-1}^{(k)}$. Recursively applying Eq. 19 yields:

$$\|\delta_{t-1}^{(k)}\| \leq L^k \|\delta_{t-1}^{(0)}\| + C \frac{1 - L^k}{1 - L}. \quad (19)$$

As $k \rightarrow \infty$, $L^k \rightarrow 0$, and the error converges to:

$$\|\delta_{t-1}^{(\infty)}\| \leq \frac{C}{1 - L}. \quad (20)$$

This result demonstrates that IEC effectively suppresses error accumulation by ensuring that the propagated error at each timestep is bounded by $\frac{C}{1 - L}$. Crucially, since IEC eliminates dependency on errors from previous timesteps, the total accumulated error after T timesteps grows only linearly: $\delta_0^{\text{IEC}} = \sum_{j=1}^T \delta_j^x$, where each δ_j^x is independently bounded. Thus, IEC can prevent exponential error amplification and achieve linear error propagation in theory. In practice, we set the maximum iteration K to 1 and the threshold τ to 1e-5. As shown in Fig. 2, IEC effectively reduces errors across timesteps, demonstrating its effectiveness in a real case.

4 EXPERIMENT

4.1 EXPERIMENT SETTINGS

Models, Baselines, Datasets, Metrics, and Implementation Details. All experiments are conducted using PyTorch on an NVIDIA 3090 GPU. To evaluate the effectiveness of IEC, we apply it to various diffusion models, including DDPM, LDM, and Stable Diffusion Song et al. (2020a); Rombach et al. (2022), as well as efficiency techniques such as timestep-wise network quantization Liu et al. (2024b), Deepcache Ma et al. (2024b), and CacheQuant Liu et al. (2025b), a hybrid technique combining quantization and feature caching. For model quantization, we adopt channel-wise quantization for weights and layer-wise quantization for activations, considering both W4A8 and W8A8 cases. For W4A8, local reconstruction is performed to enhance performance. For feature caching, following CacheQuant Ma et al. (2024b), the cached blocks are set to last 3, 1, and 1 blocks for DDIM, LDM,

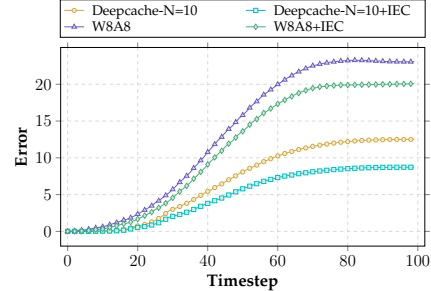
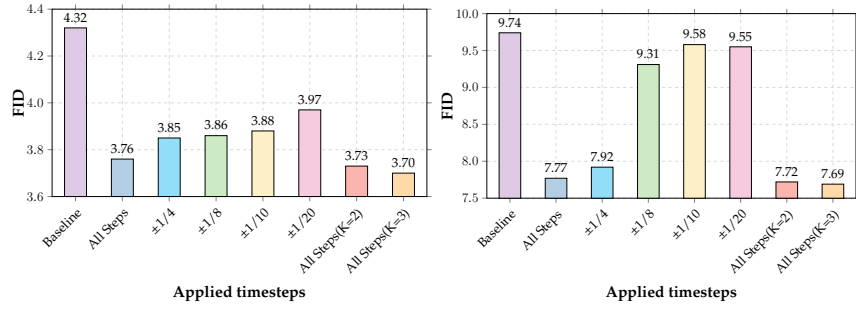


Figure 2: Error comparison across timesteps.



(a) Ablation study of applying IEC on W8A8 (b) Ablation study of applying IEC on Deepcache ($N = 10$).

Figure 3: Ablation study of applying IEC on quantization and Deepcache. The baseline does not use IEC, while ‘‘All Steps’’ applies IEC to all timesteps. The ‘‘ $\pm A$ ’’ indicates that IEC is applied to both the first and last A timesteps.

and Stable Diffusion, respectively. We evaluate IEC on several widely used datasets, including CIFAR-10 Krizhevsky et al. (2009), LSUN-Churchs Yu et al. (2015), LSUN-Bedrooms Yu et al. (2015), ImageNet Deng et al. (2009), and MS-COCO Lin et al. (2014). For Stable Diffusion, we generate 5,000 images using MS-COCO captions as prompts, following the protocols in Ma et al. (2024b); Chen et al. (2024b); Wu et al. (2024a). For all other datasets, 50,000 images are generated to evaluate the quality of image synthesis. The evaluation metrics include FID Heusel et al. (2017), Inception Score (IS) Salimans et al. (2016), and CLIP Score (evaluated on ViT-g/14) Hessel et al. (2021). For quantization-based methods, IEC is applied at every timestep. For DeepCache and CacheQuant, IEC is applied only to the non-cached timesteps, except for MS-COCO, where IEC is only applied at the first timestep. Note that IEC is applied solely to the efficient diffusion models and does not interfere with the baseline model efficiency pipelines.

Table 1: Results of combining IEC with timestep-wise quantization Liu et al. (2024b) on CIFAR-10, LSUN-Churchs, and LSUN-Bedrooms datasets.

CIFAR-10 32×32 (T=100)		LSUN-Churchs 256×256 (T=100)		LSUN-Bedrooms 256×256 (T=100)	
W/A	FID \downarrow	W/A	FID \downarrow	W/A	FID \downarrow
DDIM	4.19	LDM-8	3.99	LDM-4	3.37
W8A8	4.32	W8A8	3.57	W8A8	8.97
+IEC	3.76	+IEC	3.29	+IEC	7.78
W4A8	6.82	W4A8	6.27		
+IEC	5.96	+IEC	6.10		

4.2 ABLATION STUDY

Fig. 3 illustrates the impact of applying IEC to different subsets of timesteps. Specifically, we examine the effects of applying IEC only to the first and last timesteps, as these timesteps exhibit the largest values of $\|A_t + B_t J_t\|$ in Fig. 1a. As shown in Fig. 3a, for the W8A8 case, applying IEC to all timesteps achieves the best FID of 3.76. Notably, the performance gains remain significant even when IEC is applied to only a small number of timesteps. For instance, applying IEC to the first and last 1/10 (“ $\pm 1/10$ ”) or 1/20 (“ $\pm 1/20$ ”) of timesteps yields FID improvements of 0.44 and 0.35, respectively. These results suggest that partial application of IEC still provides meaningful benefits. A similar trend is observed in results on feature caching in Fig. 3b. Applying IEC to all timesteps improves the FID by 1.97, while employing it to the first and last 1/10 or 1/20 of timesteps leads to gains of 0.16 and 0.19, respectively. These findings demonstrate that IEC is effective and flexible, as it can be selectively applied to a subset of timesteps to balance performance improvements with

Table 2: Results of combining IEC with Deepcache Ma et al. (2024b) on CIFAR-10, LSUN-Churhcs, and LSUN-Bedrooms datasets.

CIFAR 32 × 32 (T=100)		LSUN-Churhcs 256 × 256 (T=100)		LSUN-Bedrooms 256 × 256 (T=100)	
Method	FID ↓	Method	FID ↓	Method	FID ↓
DDIM	4.19	LDM-8	3.99	LDM-4	3.37
Deepcache-N=3 +IEC	4.70 3.96	Deepcache-N=3 +IEC	5.10 4.73	Deepcache-N=2 +IEC	11.21 7.99
Deepcache-N=5 +IEC	5.73 4.83	Deepcache-N=5 +IEC	6.74 6.00	Deepcache-N=3 +IEC	11.86 8.16
Deepcache-N=10 +IEC	9.74 7.77	Deepcache-N=10 +IEC	14.81 13.17	Deepcache-N=5 +IEC	14.28 9.20
Deepcache-N=15 +IEC	17.21 14.58	Deepcache-N=15 +IEC	25.27 22.42	Deepcache-N=10 +IEC	26.09 16.91

computational cost¹. Moreover, increasing the number of correction iterations (e.g., K = 2 or K = 3) leads to marginal improvements, indicating that IEC is already effective even with a single correction step.

Table 3: Results of combining IEC with CacheQuant Liu et al. (2025b) (Denoted as CacheQ) on CIFAR-10, LSUN-Churhcs, and LSUN-Bedrooms datasets.

W/A	CIFAR-10 32 × 32 (T=100)		LSUN-Churhcs 256 × 256 (T=100)		W/A	LSUN-Bedrooms 256 × 256 (T=100)	
	Method	FID ↓	Method	FID ↓		Method	FID ↓
	DDIM	4.19	LDM-8	3.99		LDM-4	3.37
8/8	CacheQ-N=3 +IEC	4.61 3.93	CacheQ-N=3 +IEC	3.66 3.39	4/8	CacheQ-N=2 +IEC	8.85 7.51
	CacheQ-N=5 +IEC	5.28 5.09	CacheQ-N=5 +IEC	3.71 3.24		CacheQ-N=3 +IEC	9.27 7.33
	CacheQ-N=10 +IEC	8.19 6.47	CacheQ-N=10 +IEC	5.54 4.25		CacheQ-N=5 +IEC	10.29 7.67
	CacheQ-N=15 +IEC	13.42 10.77	CacheQ-N=15 +IEC	9.47 6.90		CacheQ-N=10 +IEC	17.53 11.07
4/8	CacheQ-N=3 +IEC	7.27 6.42	CacheQ-N=3 +IEC	7.08 6.85			
	CacheQ-N=5 +IEC	8.15 6.90	CacheQ-N=5 +IEC	7.24 6.79			
	CacheQ-N=10 +IEC	11.36 10.69	CacheQ-N=10 +IEC	10.75 9.69			
	CacheQ-N=15 +IEC	16.76 15.50	CacheQ-N=15 +IEC	13.28 11.50			

4.3 MAIN RESULTS

This subsection includes the quantitative results, while the visualizations are included in the appendix.

Evaluation on IEC on Network Quantization. Tab. 1 presents the quantization performance. For LSUN-Bedrooms, we report only W8A8 results, as W4A8 quantization leads to model collapse.

¹In Sec. A.1, we provide discussion about the time overhead of IEC.

Across all datasets, applying IEC consistently improves performance. For example, in the W4A8 case, IEC reduces the FID from 6.82 to 5.96 on CIFAR-10, and from 6.27 to 6.10 on LSUN-Churhcs.

Evaluation on IEC on Feature Caching. The performance of IEC on DeepCache Ma et al. (2024b) is shown in Tab. 2, demonstrating consistent improvements. For example, on CIFAR-10, IEC reduces FID from 4.70 to 3.96 when $N = 3$. Similar trends are observed for larger N , with FID reduced from 17.21 to 14.58 when $N = 15$. On LSUN-Churhcs, IEC reduces FID from 25.27 to 22.42 at $N = 15$, and on LSUN-Bedrooms, from 26.09 to 16.91 at $N = 10$.

Combined With Quantization-Caching. The results of IEC on CacheQuant Liu et al. (2025b), which integrates quantization and feature caching, are shown in Tab. 3 and Tab. 4. On CIFAR-10, IEC achieves consistent improvements. For instance, under W8A8 with $N = 3$, FID is reduced from 4.61 to 3.93. With $N = 15$, FID improves from 13.42 to 10.77. Similar improvements are observed under W4A8. For example, at $N = 10$, FID improves from 11.36 to 10.69. On LSUN-Churhcs, for W8A8 and $N = 3$, IEC reduces FID from 3.66 to 3.39. At $N = 15$, FID drops from 9.47 to 6.90. Under W4A8, IEC improves FID by 0.23, 0.45, 1.06, and 1.78 for $N = 3, 5, 10$, and 15, respectively. On LSUN-Bedrooms, IEC also provides consistent gains. For example, under W8A8 with $N = 2$, FID improves from 8.85 to 7.51. As shown in Tab. 4, on ImageNet, IEC enhances performance across all baselines. For instance, under W8A8 with $N = 10$, FID improves from 4.68 to 4.15 and IS from 184.38 to 196.20. At $N = 20$, FID decreases from 7.21 to 6.53, and IS increases from 160.68 to 169.71. Under W4A8, IEC also improves performance. For example, at $N = 10$, FID improves from 6.90 to 6.50 and IS from 158.27 to 161.86, demonstrating IEC’s robustness in low-precision scenarios. On MS-COCO, IEC also brings improvements. For example, under W8A8 with $N = 10$, FID improves from 23.65 to 23.36, IS from 36.71 to 37.02, and CLIP Score from 26.41 to 26.45. At $N = 5$, FID improves from 23.74 to 22.83, IS from 39.81 to 40.91, and CLIP Score from 26.87 to 26.94.

In summary, across all datasets and efficiency techniques, the integration of IEC consistently enhances performance, demonstrating its effectiveness.

Table 4: Results of combining IEC with CacheQuant Liu et al. (2025b) (Denoted as CacheQ) on ImageNet and MS-COCO datasets.

		ImageNet 256 × 25 (T=250)					MS-COCO 256 × 256 (T=50)		
		Method	FID ↓	IS ↑	W/A	Method	FID ↓	IS ↑	CLIP Score ↑
8/8	LDM-4		3.37	204.56	8/8	PLMS	22.41	41.02	26.89
	CacheQ-N=10 +IEC	4.68 4.15	184.38 196.20			CacheQ-N=10 +IEC	23.65 23.36	36.71 37.02	26.41 26.45
	CacheQ-N=15 +IEC	5.51 5.18	174.81 182.30			CacheQ-N=5 +IEC	23.74 22.83	39.81 40.91	26.87 26.94
	CacheQ-N=20 +IEC	7.21 6.53	160.68 169.71			CacheQ-N=10 +IEC	26.63 24.82	34.57 36.18	26.23 26.25
	CacheQ-N=10 +IEC	6.90 6.50	158.27 161.86			CacheQ-N=5 +IEC	23.85 23.80	39.53 40.27	26.78 26.80
	CacheQ-N=15 +IEC	9.40 8.66	139.64 144.41						
4/8	CacheQ-N=20 +IEC	12.65 11.10	124.13 130.01						

5 DISCUSSION

The analysis in Sec. 3.1 suggests that more robust models can be achieved by modifying the scheduling schemes of A_t and B_t , or by explicitly fine-tuning the model to control the norm of the Jacobian. Additionally, as discussed in Sec. 4.2, identifying a small subset of critical timesteps for applying the proposed IEC can significantly reduce inference overhead while still improving generation quality. Finally, this paper presents a conceptual and experimental validation of the test-time method for

diffusion, while further exploring other diffusion models, samplers, and efficiency techniques remains an interesting topic. Although these directions are promising, we leave their exploration to future work due to current resource limitations.

6 CONCLUSION

In this paper, we address the challenge of improving the performance of efficient diffusion models at test-time. We begin by analyzing the error accumulation in such models and show that these errors can grow exponentially during the denoising process. To mitigate this, we introduce Iterative Error Correction (IEC), a simple yet effective method that iteratively refines the model’s output to suppress error propagation. Our theoretical analysis demonstrates that IEC converges to a fixed-point solution, reducing the rate of error growth from exponential to linear. As a plug-and-play, model-agnostic method, IEC offers a flexible trade-off between performance and efficiency, allowing users to adapt it to various practical scenarios. We validate IEC through extensive experiments, showing consistent performance gains across various datasets, efficiency techniques, and diffusion model architectures.

REFERENCES

Omri Avrahami, Dani Lischinski, and Ohad Fried. Blended diffusion for text-driven editing of natural images. In *Proceedings of the IEEE/CVF conference on computer vision and pattern recognition*, pp. 18208–18218, 2022.

Stefan Banach. Sur les opérations dans les ensembles abstraits et leur application aux équations intégrales. *Fundamenta Mathematicae*, 3(1):133–181, 1922.

Lei Chen, Yuan Meng, Chen Tang, Xinzhu Ma, Jingyan Jiang, Xin Wang, Zhi Wang, and Wenwu Zhu. Q-dit: Accurate post-training quantization for diffusion transformers. *arXiv preprint arXiv:2406.17343*, 2024a.

Pengtao Chen, Mingzhu Shen, Peng Ye, Jianjian Cao, Chongjun Tu, Christos-Savvas Bouganis, Yiren Zhao, and Tao Chen. Delta-dit: A training-free acceleration method tailored for diffusion transformers. *arXiv preprint arXiv:2406.01125*, 2024b.

Jooyoung Choi, Sungwon Kim, Yonghyun Jeong, Youngjune Gwon, and Sungroh Yoon. Ilvr: Conditioning method for denoising diffusion probabilistic models. *arXiv preprint arXiv:2108.02938*, 2021.

Jia Deng, Wei Dong, Richard Socher, Li-Jia Li, Kai Li, and Li Fei-Fei. Imagenet: A large-scale hierarchical image database. In *2009 IEEE conference on computer vision and pattern recognition*, pp. 248–255. Ieee, 2009.

Juncan Deng, Shuaiting Li, Zeyu Wang, Hong Gu, Kedong Xu, and Kejie Huang. Vq4dit: Efficient post-training vector quantization for diffusion transformers. In *Proceedings of the AAAI Conference on Artificial Intelligence*, volume 39, pp. 16226–16234, 2025.

Tim Dockhorn, Arash Vahdat, and Karsten Kreis. Genie: Higher-order denoising diffusion solvers. *Advances in Neural Information Processing Systems*, 35:30150–30166, 2022.

Zhenyuan Dong and Sai Qian Zhang. Ditas: Quantizing diffusion transformers via enhanced activation smoothing. In *2025 IEEE/CVF Winter Conference on Applications of Computer Vision (WACV)*, pp. 4606–4615. IEEE, 2025.

Zichen Fan, Steve Dai, Rangharajan Venkatesan, Dennis Sylvester, and Brucek Khailany. Sq-dm: Accelerating diffusion models with aggressive quantization and temporal sparsity. *arXiv preprint arXiv:2501.15448*, 2025.

Gongfan Fang, Kunjun Li, Xinyin Ma, and Xinchao Wang. Tinyfusion: Diffusion transformers learned shallow. *arXiv preprint arXiv:2412.01199*, 2024.

Weilun Feng, Haotong Qin, Chuanguang Yang, Zhulin An, Libo Huang, Boyu Diao, Fei Wang, Renshuai Tao, Yongjun Xu, and Michele Magno. Mpq-dm: Mixed precision quantization for extremely low bit diffusion models. In *Proceedings of the AAAI Conference on Artificial Intelligence*, volume 39, pp. 16595–16603, 2025.

Sicheng Gao, Xuhui Liu, Bohan Zeng, Sheng Xu, Yanjing Li, Xiaoyan Luo, Jianzhuang Liu, Xiantong Zhen, and Baochang Zhang. Implicit diffusion models for continuous super-resolution. In *Proceedings of the IEEE/CVF conference on computer vision and pattern recognition*, pp. 10021–10030, 2023.

Yefei He, Jing Liu, Weijia Wu, Hong Zhou, and Bohan Zhuang. Efficientdm: Efficient quantization-aware fine-tuning of low-bit diffusion models. *arXiv preprint arXiv:2310.03270*, 2023.

Yefei He, Luping Liu, Jing Liu, Weijia Wu, Hong Zhou, and Bohan Zhuang. Ptqd: Accurate post-training quantization for diffusion models. *Advances in Neural Information Processing Systems*, 36, 2024.

Jack Hessel, Ari Holtzman, Maxwell Forbes, Ronan Le Bras, and Yejin Choi. Clipscore: A reference-free evaluation metric for image captioning. *arXiv preprint arXiv:2104.08718*, 2021.

Martin Heusel, Hubert Ramsauer, Thomas Unterthiner, Bernhard Nessler, and Sepp Hochreiter. Gans trained by a two time-scale update rule converge to a local nash equilibrium. *Advances in neural information processing systems*, 30, 2017.

Jonathan Ho, Ajay Jain, and Pieter Abbeel. Denoising diffusion probabilistic models. *Advances in neural information processing systems*, 33:6840–6851, 2020.

Edward J Hu, Yelong Shen, Phillip Wallis, Zeyuan Allen-Zhu, Yuanzhi Li, Shean Wang, Lu Wang, and Weizhu Chen. Lora: Low-rank adaptation of large language models. *arXiv preprint arXiv:2106.09685*, 2021.

Rongjie Huang, Zhou Zhao, Huadai Liu, Jinglin Liu, Chenye Cui, and Yi Ren. Prodif: Progressive fast diffusion model for high-quality text-to-speech. In *Proceedings of the 30th ACM International Conference on Multimedia*, pp. 2595–2605, 2022.

Yushi Huang, Ruihao Gong, Jing Liu, Tianlong Chen, and Xianglong Liu. Tfmq-dm: Temporal feature maintenance quantization for diffusion models. In *Proceedings of the IEEE/CVF Conference on Computer Vision and Pattern Recognition (CVPR)*, pp. 7362–7371, June 2024a.

Yushi Huang, Ruihao Gong, Jing Liu, Tianlong Chen, and Xianglong Liu. Tfmq-dm: Temporal feature maintenance quantization for diffusion models. In *Proceedings of the IEEE/CVF Conference on Computer Vision and Pattern Recognition*, pp. 7362–7371, 2024b.

Bahjat Kawar, Shiran Zada, Oran Lang, Omer Tov, Huiwen Chang, Tali Dekel, Inbar Mosseri, and Michal Irani. Imagic: Text-based real image editing with diffusion models. In *Proceedings of the IEEE/CVF Conference on Computer Vision and Pattern Recognition*, pp. 6007–6017, 2023.

Alex Krizhevsky, Geoffrey Hinton, et al. Learning multiple layers of features from tiny images. 2009.

Haoying Li, Yifan Yang, Meng Chang, Shiqi Chen, Huajun Feng, Zhihai Xu, Qi Li, and Yueting Chen. Srdiff: Single image super-resolution with diffusion probabilistic models. *Neurocomputing*, 479:47–59, 2022.

Muyang Li, Tianle Cai, Jiaxin Cao, Qinsheng Zhang, Han Cai, Junjie Bai, Yangqing Jia, Kai Li, and Song Han. Distrifusion: Distributed parallel inference for high-resolution diffusion models. In *Proceedings of the IEEE/CVF Conference on Computer Vision and Pattern Recognition*, pp. 7183–7193, 2024a.

Muyang Li, Yujun Lin, Zhekai Zhang, Tianle Cai, Junxian Guo, Xiuyu Li, Enze Xie, Chenlin Meng, Jun-Yan Zhu, and Song Han. Svdquant: Absorbing outliers by low-rank component for 4-bit diffusion models. In *The Thirteenth International Conference on Learning Representations*, 2024b.

Xiuyu Li, Yijiang Liu, Long Lian, Huanrui Yang, Zhen Dong, Daniel Kang, Shanghang Zhang, and Kurt Keutzer. Q-diffusion: Quantizing diffusion models. In *Proceedings of the IEEE/CVF International Conference on Computer Vision*, pp. 17535–17545, 2023.

Yanjing Li, Sheng Xu, Xianbin Cao, Xiao Sun, and Baochang Zhang. Q-dm: An efficient low-bit quantized diffusion model. *Advances in Neural Information Processing Systems*, 36, 2024c.

Hunter Lightman, Vineet Kosaraju, Yuri Burda, Harrison Edwards, Bowen Baker, Teddy Lee, Jan Leike, John Schulman, Ilya Sutskever, and Karl Cobbe. Let’s verify step by step. In *The Twelfth International Conference on Learning Representations*, 2023.

Chen-Hsuan Lin, Jun Gao, Luming Tang, Towaki Takikawa, Xiaohui Zeng, Xun Huang, Karsten Kreis, Sanja Fidler, Ming-Yu Liu, and Tsung-Yi Lin. Magic3d: High-resolution text-to-3d content creation. In *Proceedings of the IEEE/CVF Conference on Computer Vision and Pattern Recognition*, pp. 300–309, 2023.

Tsung-Yi Lin, Michael Maire, Serge Belongie, James Hays, Pietro Perona, Deva Ramanan, Piotr Dollár, and C Lawrence Zitnick. Microsoft coco: Common objects in context. In *Computer Vision–ECCV 2014: 13th European Conference, Zurich, Switzerland, September 6–12, 2014, Proceedings, Part V 13*, pp. 740–755. Springer, 2014.

Feng Liu, Shiwei Zhang, Xiaofeng Wang, Yujie Wei, Haonan Qiu, Yuzhong Zhao, Yingya Zhang, Qixiang Ye, and Fang Wan. Timestep embedding tells: It’s time to cache for video diffusion model. *arXiv preprint arXiv:2411.19108*, 2024a.

Jiacheng Liu, Chang Zou, Yuanhuiyi Lyu, Junjie Chen, and Linfeng Zhang. From reusing to forecasting: Accelerating diffusion models with taylorseers. *arXiv preprint arXiv:2503.06923*, 2025a.

Luping Liu, Yi Ren, Zhijie Lin, and Zhou Zhao. Pseudo numerical methods for diffusion models on manifolds. *arXiv preprint arXiv:2202.09778*, 2022.

Xuewen Liu, Zhikai Li, and Qingyi Gu. Dilatequant: Accurate and efficient diffusion quantization via weight dilation. *arXiv preprint arXiv:2409.14307*, 2024b.

Xuewen Liu, Zhikai Li, Junrui Xiao, and Qingyi Gu. Enhanced distribution alignment for post-training quantization of diffusion models. *arXiv e-prints*, pp. arXiv–2401, 2024c.

Xuewen Liu, Zhikai Li, and Qingyi Gu. Cachequant: Comprehensively accelerated diffusion models. *arXiv preprint arXiv:2503.01323*, 2025b.

Cheng Lu, Yuhao Zhou, Fan Bao, Jianfei Chen, Chongxuan Li, and Jun Zhu. Dpm-solver: A fast ode solver for diffusion probabilistic model sampling in around 10 steps. *Advances in Neural Information Processing Systems*, 35:5775–5787, 2022a.

Cheng Lu, Yuhao Zhou, Fan Bao, Jianfei Chen, Chongxuan Li, and Jun Zhu. Dpm-solver++: Fast solver for guided sampling of diffusion probabilistic models. *arXiv preprint arXiv:2211.01095*, 2022b.

Shitong Luo and Wei Hu. Diffusion probabilistic models for 3d point cloud generation. In *Proceedings of the IEEE/CVF conference on computer vision and pattern recognition*, pp. 2837–2845, 2021.

Nanye Ma, Shangyuan Tong, Haolin Jia, Hexiang Hu, Yu-Chuan Su, Mingda Zhang, Xuan Yang, Yandong Li, Tommi Jaakkola, Xuhui Jia, et al. Inference-time scaling for diffusion models beyond scaling denoising steps. *arXiv preprint arXiv:2501.09732*, 2025.

Xinyin Ma, Gongfan Fang, Michael Bi Mi, and Xinchao Wang. Learning-to-cache: Accelerating diffusion transformer via layer caching, 2024a.

Xinyin Ma, Gongfan Fang, and Xinchao Wang. Deepcache: Accelerating diffusion models for free. In *Proceedings of the IEEE/CVF conference on computer vision and pattern recognition*, pp. 15762–15772, 2024b.

Kangfu Mei and Vishal Patel. Vidm: Video implicit diffusion models. In *Proceedings of the AAAI conference on artificial intelligence*, volume 37, pp. 9117–9125, 2023.

Chenlin Meng, Yutong He, Yang Song, Jiaming Song, Jiajun Wu, Jun-Yan Zhu, and Stefano Ermon. Sdedit: Guided image synthesis and editing with stochastic differential equations. *arXiv preprint arXiv:2108.01073*, 2021.

Niklas Muennighoff, Zitong Yang, Weijia Shi, Xiang Lisa Li, Li Fei-Fei, Hannaneh Hajishirzi, Luke Zettlemoyer, Percy Liang, Emmanuel Candès, and Tatsunori Hashimoto. s1: Simple test-time scaling. *arXiv preprint arXiv:2501.19393*, 2025.

James R Munkres. *Analysis on manifolds*. CRC Press, 2018.

Alex Nichol, Prafulla Dhariwal, Aditya Ramesh, Pranav Shyam, Pamela Mishkin, Bob McGrew, Ilya Sutskever, and Mark Chen. Glide: Towards photorealistic image generation and editing with text-guided diffusion models. *arXiv preprint arXiv:2112.10741*, 2021.

Alexander Quinn Nichol and Prafulla Dhariwal. Improved denoising diffusion probabilistic models. In *International conference on machine learning*, pp. 8162–8171. PMLR, 2021.

Ben Poole, Ajay Jain, Jonathan T Barron, and Ben Mildenhall. Dreamfusion: Text-to-3d using 2d diffusion. *arXiv preprint arXiv:2209.14988*, 2022.

Mihir Prabhudesai, Tsung-Wei Ke, Alex Li, Deepak Pathak, and Katerina Fragkiadaki. Diffusion-tta: Test-time adaptation of discriminative models via generative feedback. *Advances in Neural Information Processing Systems*, 36:17567–17583, 2023.

Aditya Ramesh, Prafulla Dhariwal, Alex Nichol, Casey Chu, and Mark Chen. Hierarchical text-conditional image generation with clip latents. *arXiv preprint arXiv:2204.06125*, 1(2):3, 2022.

Robin Rombach, Andreas Blattmann, Dominik Lorenz, Patrick Esser, and Björn Ommer. High-resolution image synthesis with latent diffusion models. In *Proceedings of the IEEE/CVF conference on computer vision and pattern recognition*, pp. 10684–10695, 2022.

Chitwan Saharia, William Chan, Huiwen Chang, Chris Lee, Jonathan Ho, Tim Salimans, David Fleet, and Mohammad Norouzi. Palette: Image-to-image diffusion models. In *ACM SIGGRAPH 2022 conference proceedings*, pp. 1–10, 2022a.

Chitwan Saharia, William Chan, Saurabh Saxena, Lala Li, Jay Whang, Emily L Denton, Kamyar Ghasemipour, Raphael Gontijo Lopes, Burcu Karagol Ayan, Tim Salimans, et al. Photorealistic text-to-image diffusion models with deep language understanding. *Advances in neural information processing systems*, 35:36479–36494, 2022b.

Chitwan Saharia, Jonathan Ho, William Chan, Tim Salimans, David J Fleet, and Mohammad Norouzi. Image super-resolution via iterative refinement. *IEEE transactions on pattern analysis and machine intelligence*, 45(4):4713–4726, 2022c.

Tim Salimans, Ian Goodfellow, Wojciech Zaremba, Vicki Cheung, Alec Radford, and Xi Chen. Improved techniques for training gans. *Advances in neural information processing systems*, 29, 2016.

Yuzhang Shang, Zhihang Yuan, Bin Xie, Bingzhe Wu, and Yan Yan. Post-training quantization on diffusion models. In *Proceedings of the IEEE/CVF conference on computer vision and pattern recognition*, pp. 1972–1981, 2023.

Andy Shih, Suneel Belkhale, Stefano Ermon, Dorsa Sadigh, and Nima Anari. Parallel sampling of diffusion models. *Advances in Neural Information Processing Systems*, 36:4263–4276, 2023.

Raghav Singhal, Zachary Horvitz, Ryan Teehan, Mengye Ren, Zhou Yu, Kathleen McKeown, and Rajesh Ranganath. A general framework for inference-time scaling and steering of diffusion models. *arXiv preprint arXiv:2501.06848*, 2025.

Charlie Snell, Jaehoon Lee, Kelvin Xu, and Aviral Kumar. Scaling llm test-time compute optimally can be more effective than scaling model parameters. *arXiv preprint arXiv:2408.03314*, 2024.

Jiaming Song, Chenlin Meng, and Stefano Ermon. Denoising diffusion implicit models. *arXiv preprint arXiv:2010.02502*, 2020a.

Yang Song, Jascha Sohl-Dickstein, Diederik P Kingma, Abhishek Kumar, Stefano Ermon, and Ben Poole. Score-based generative modeling through stochastic differential equations. *arXiv preprint arXiv:2011.13456*, 2020b.

Haojun Sun, Chen Tang, Zhi Wang, Yuan Meng, Xinzhu Ma, Wenwu Zhu, et al. Tmpq-dm: Joint timestep reduction and quantization precision selection for efficient diffusion models. *arXiv preprint arXiv:2404.09532*, 2024.

Narek Tumanyan, Michal Geyer, Shai Bagon, and Tali Dekel. Plug-and-play diffusion features for text-driven image-to-image translation. In *Proceedings of the IEEE/CVF Conference on Computer Vision and Pattern Recognition*, pp. 1921–1930, 2023.

Changyuan Wang, Ziwei Wang, Xiuwei Xu, Yansong Tang, Jie Zhou, and Jiwen Lu. Towards accurate post-training quantization for diffusion models. *arXiv preprint arXiv:2305.18723*, 2023.

Changyuan Wang, Ziwei Wang, Xiuwei Xu, Yansong Tang, Jie Zhou, and Jiwen Lu. Towards accurate post-training quantization for diffusion models. In *Proceedings of the IEEE/CVF Conference on Computer Vision and Pattern Recognition*, pp. 16026–16035, 2024a.

Haoxuan Wang, Yuzhang Shang, Zhihang Yuan, Junyi Wu, and Yan Yan. Quest: Low-bit diffusion model quantization via efficient selective finetuning. *arXiv preprint arXiv:2402.03666*, 2024b.

Felix Wimbauer, Bichen Wu, Edgar Schoenfeld, Xiaoliang Dai, Ji Hou, Zijian He, Artsiom Sanakoyeu, Peizhao Zhang, Sam Tsai, Jonas Kohler, et al. Cache me if you can: Accelerating diffusion models through block caching. In *Proceedings of the IEEE/CVF Conference on Computer Vision and Pattern Recognition*, pp. 6211–6220, 2024.

Junyi Wu, Haoxuan Wang, Yuzhang Shang, Mubarak Shah, and Yan Yan. Ptq4dit: Post-training quantization for diffusion transformers. *arXiv preprint arXiv:2405.16005*, 2024a.

Junyi Wu, Haoxuan Wang, Yuzhang Shang, Mubarak Shah, and Yan Yan. Ptq4dit: Post-training quantization for diffusion transformers. In *Advances in Neural Information Processing Systems*, 2024b.

Zehao Xiao and Cees GM Snoek. Beyond model adaptation at test time: A survey. *arXiv preprint arXiv:2411.03687*, 2024.

Yuewei Yang, Jialiang Wang, Xiaoliang Dai, Peizhao Zhang, and Hongbo Zhang. An analysis on quantizing diffusion transformers. *arXiv preprint arXiv:2406.11100*, 2024.

Tianwei Yin, Michaël Gharbi, Taesung Park, Richard Zhang, Eli Shechtman, Fredo Durand, and Bill Freeman. Improved distribution matching distillation for fast image synthesis. *Advances in neural information processing systems*, 37:47455–47487, 2024a.

Tianwei Yin, Michaël Gharbi, Richard Zhang, Eli Shechtman, Fredo Durand, William T Freeman, and Taesung Park. One-step diffusion with distribution matching distillation. In *Proceedings of the IEEE/CVF conference on computer vision and pattern recognition*, pp. 6613–6623, 2024b.

Fisher Yu, Ari Seff, Yinda Zhang, Shuran Song, Thomas Funkhouser, and Jianxiong Xiao. Lsun: Construction of a large-scale image dataset using deep learning with humans in the loop. *arXiv preprint arXiv:1506.03365*, 2015.

Chenshuang Zhang, Chaoning Zhang, Sheng Zheng, Mengchun Zhang, Maryam Qamar, Sung-Ho Bae, and In So Kweon. A survey on audio diffusion models: Text to speech synthesis and enhancement in generative ai. *arXiv preprint arXiv:2303.13336*, 2023a.

Lvmin Zhang, Anyi Rao, and Maneesh Agrawala. Adding conditional control to text-to-image diffusion models. In *Proceedings of the IEEE/CVF International Conference on Computer Vision*, pp. 3836–3847, 2023b.

Qinsheng Zhang, Molei Tao, and Yongxin Chen. gddim: Generalized denoising diffusion implicit models. *arXiv preprint arXiv:2206.05564*, 2022.

Tianchen Zhao, Tongcheng Fang, Enshu Liu, Wan Rui, Widya Dewi Soedarmadji, Shiyao Li, Zinan Lin, Guohao Dai, Shengen Yan, Huazhong Yang, Xuefei Ning, and Yu Wang. Vudit-q: Efficient and accurate quantization of diffusion transformers for image and video generation, 2024.

Hongkai Zheng, Weili Nie, Arash Vahdat, Kamyar Azizzadenesheli, and Anima Anandkumar. Fast sampling of diffusion models via operator learning. In *International conference on machine learning*, pp. 42390–42402. PMLR, 2023.

Xingyu Zheng, Haotong Qin, Xudong Ma, Mingyuan Zhang, Haojie Hao, Jiakai Wang, Zixiang Zhao, Jinyang Guo, and Xianglong Liu. Binarydm: Towards accurate binarization of diffusion model. *arXiv preprint arXiv:2404.05662*, 2024.

Chang Zou, Xuyang Liu, Ting Liu, Siteng Huang, and Linfeng Zhang. Accelerating diffusion transformers with token-wise feature caching. *arXiv preprint arXiv:2410.05317*, 2024.

A APPENDIX

A.1 OVERHEAD DISCUSSION

Table 5 presents the overhead and FID when combining our IEC with timestep-wise quantization Liu et al. (2024b) and Deepcache Ma et al. (2024b) on the CIFAR-10 dataset. Here, we measure the time overhead by comparing it with the baseline without IEC. For W8A8 quantization, IEC achieves substantial improvements in FID with minimal overhead. For instance, selectively applying IEC to $\pm 1/10$ or $\pm 1/20$ of the steps achieves improved FID of 3.88 and 3.97 with only 20% and 10% overhead, respectively. In the case of DeepCache, the IEC is only applied to the non-cached timesteps, thereby its overhead is minimal. For example, applying IEC to all timesteps yields a FID of 7.77 with only 14% overhead, while applying IEC to $\pm 1/10$ or $\pm 1/20$ reduces the FID to 9.58 and 9.55, respectively, with overheads as low as 2.8% and 1.4%. These results demonstrate that IEC provides a flexible trade-off between efficiency and generation quality, making it easy to use and suitable for real-world applications.

Table 5: Overhead of combining IEC with timestep-wise quantization Liu et al. (2024b) and Deepcache (N=10) Ma et al. (2024b) on CIFAR-10.

CIFAR-10 32 × 32 (T=100)			CIFAR-10 32 × 32 (T=100)		
W/A	FID ↓	Time Overhead	Method	FID ↓	Time Overhead
DDIM	4.19	-	DDIM	4.19	-
W8A8	4.32	0%	Deepcache-N=10	9.74	0%
All Step (K=1)	3.76	100%	All Step (K=1)	7.77	14%
$\pm 1/4$	3.85	50%	$\pm 1/4$	7.92	7%
$\pm 1/8$	3.86	25%	$\pm 1/8$	9.31	4.2%
$\pm 1/10$	3.88	20%	$\pm 1/10$	9.58	2.8%
$\pm 1/20$	3.97	10%	$\pm 1/20$	9.55	1.4%

A.2 VISUALIZATION

In this section, we provide visualization comparisons between the proposed IEC and the corresponding baseline. Fig. 4 and Fig. 5 show the visualization results of Stable Diffusion on the COCO dataset. Fig. 6, Fig. 7, and Fig. 8 show the visualization results of LDM-8 on the LSUN-Churchs datasets. Fig. 9, Fig. 10, and Fig. 11 show the visualization results of LDM-4 on the LSUN-Bedrooms datasets.

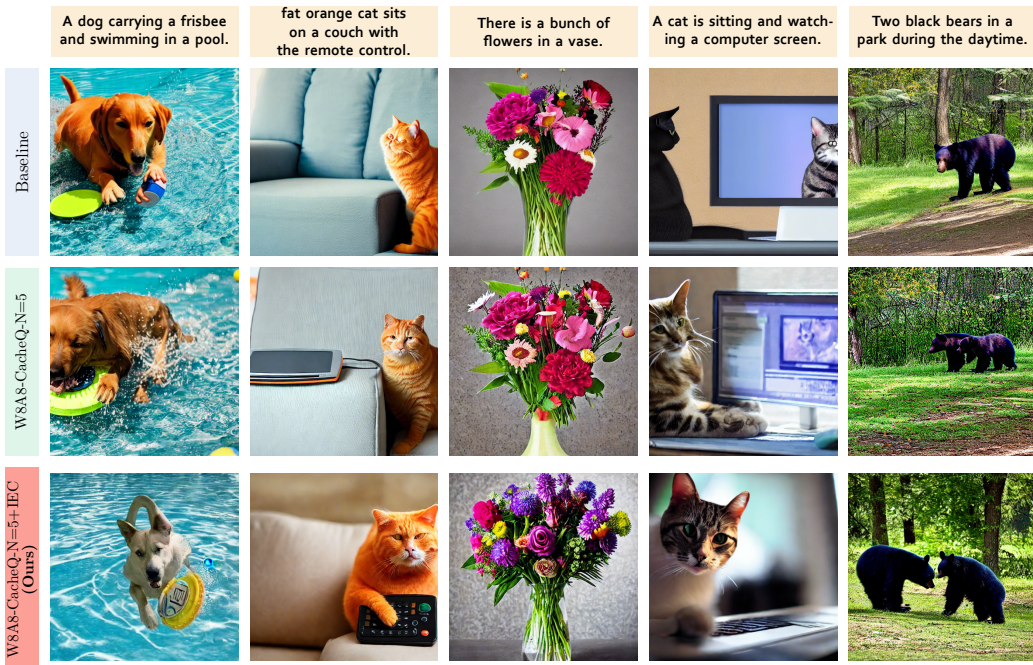


Figure 4: Qualitative comparison of Stable Diffusion on the COCO dataset: Baseline vs. CacheQuant (W8A8, N=5) with and without IEC.

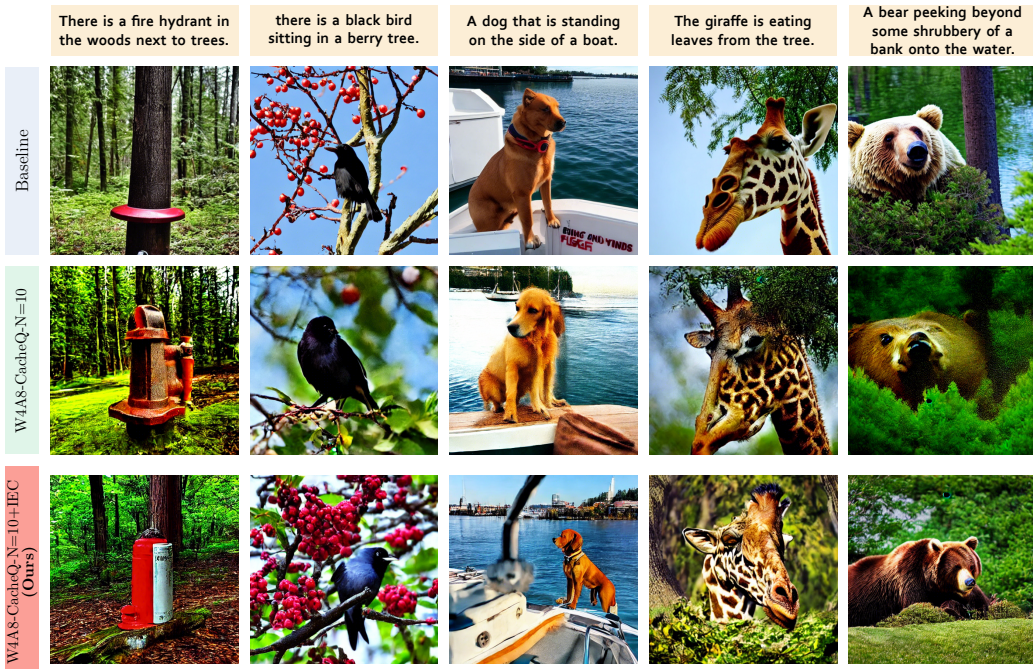


Figure 5: Qualitative comparison of Stable Diffusion on the COCO dataset: Baseline vs. CacheQuant (W4A8, N=10) with and without IEC.



Figure 6: Qualitative comparison of LDM-8 on the LSUN-Churchs dataset: W8A8 vs. W8A8+IEC.



Figure 7: Qualitative comparison of LDM-8 on the LSUN-Churchs dataset: DeepCache (N=10) vs. DeepCache+IEC (N=10) .



Figure 8: Qualitative comparison of LDM-8 on the LSUN-Churchs dataset: CacheQuant (W8A8, N=10) vs. CacheQuant+IEC (W8A8, N=10) .



Figure 9: Qualitative comparison of LDM-4 on the LSUN-Bedrooms dataset: W8A8 vs. W8A8+IEC.

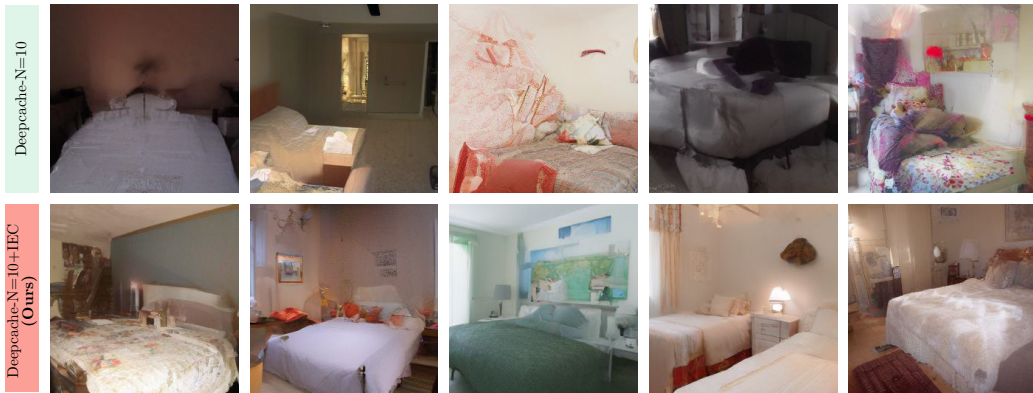


Figure 10: Qualitative comparison of LDM-4 on the LSUN-Bedrooms dataset: DeepCache (N=10) vs. DeepCache+IEC (N=10) .



Figure 11: Qualitative comparison of LDM-4 on the LSUN-Bedrooms dataset: CacheQuant (W8A8, N=10) vs. CacheQuant+IEC (W8A8, N=10) .